Resonant inelastic scattering of quasifree electrons on $C^{5+}(1s)$

P. Hvelplund, A. D. González,* P. Dahl, and C. P. Bhalla†
Institute of Physics and Astronomy, Aarhus University, DK-8000 Aarhus C, Denmark
(Received 21 September 1993)

We report on studies of resonant inelastic scattering of quasifree electrons on C^{5+}. The resolution of the electron spectrometer is sufficient to resolve the energy structure of electrons emitted as a result of decay of doubly excited $3l3l'$ configurations in C^{4+}. The line energies compare well with theoretical calculations, using the truncated-diagonalization method. Theoretical calculations based on the Hartree-Fock atomic model for the differential cross sections are also presented. The relative strength of these states within the $3l3l'$ manifold is measured as a function of scattering angle and compared with theory. The agreement is good for several states, but the $3s3d\ ^3D$ and $3p3d\ ^1F$ states show large deviations from the Hartree-Fock-model calculations. Good agreement is found between theory and experimental data for the ^1F state when the autoionization rate to the ground state calculated with the truncated-diagonalization method is used in the calculations. It is likely that strong correlation effects for the ^3D state are not as well treated in the Hartree-Fock model as by the truncated-diagonalization method.

PACS number(s): 34.50.Fa

I. INTRODUCTION

During recent years, elastic scattering of quasifree electrons on energetic ions has been studied both experimentally [1] and theoretically [2]. Several studies of resonances in the elastic-scattering cross section have also been reported, usually under the name of resonant-transfer excitation Auger emission (RTEA) [3,4]. Excitation of the projectile electron by the transferred target electron is normally the dominant excitation mechanism [5]. These so-called quasifree electrons are originally bound in the target atom, but since their binding energy is small compared with their kinetic energy in the projectile system, we may consider them as free. The energy distribution of these electrons or the "target temperature" is determined via the Compton profile of the target electron. In RTEA studies, the resonances are attributed to the population of an intermediate state, which then decays via Auger emission.

A characteristic feature in resonant elastic scattering is that the initial and final ion states are identical such as in the process $C^{5+}(1s)+e\rightarrow C^{4+}(2l,nl')\rightarrow C^{5+}(1s)+e$. Resonant scattering of electrons on one-electron ions is reported by De Paola, Parameswaran, and Axmann [6], and Schulz *et al.* [7], and calculations are performed by Badnell [4] and Bhalla [8]. The process, where the intermediate two-electron state decays by radiation, results in dielectronic recombination (DR). Measurements of DR on one-electron ions are reported by Kilgus *et al.* [9], and the corresponding theory by Griffin and Pindzola [10]. For a general discussion of RTEA and DR, the reader is referred to review articles by Zouros [11], and Hahn and La Gattuta [12].

In the present paper, another step in the direction of detailed investigations of doubly excited states in ion-atom collisions is reported. The process in focus is what could be called resonant inelastic scattering of quasifree electrons. The inelasticity is related to the different initial and final ion states such as in the process $C^{5+}(1s)+e\rightarrow C^{4+}(3lnl')\rightarrow C^{5+}(2l)+e$. Measurements involving electrons emitted as a result of the decay of doubly excited $(3l,3l')$ configurations in C^{4+} populated in collisions between 8.6-MeV C^{5+} and H_2 are discussed below. Several lines in the electron spectrum are identified, and line energies and relative intensities are compared with theoretical calculations. The angular dependence of the line intensities has also been measured for laboratory angles in the range of 1°–5°.

In both resonant elastic and inelastic scattering, interference with the corresponding direct nonresonant channel is possible. The signature of such interferences is observed in the present measurements, and the related problems for a comparison of relative line intensities are discussed.

II. THEORY

The process considered in this paper is analogous to a free-electron inelastic scattering from a hydrogenlike ion. In addition to the direct inelastic process, where the initial electron $(1s)$ of the ion is excited to $2l$ states, manifolds of doubly excited heliumlike states such as $3l3l'$ that predominantly deexcite to $2l$ exist. In general, interference is found between the two processes, and one expects a Fano-type profile in the differential inelastic cross section at electron energies that can populate the doubly excited states. Here only the contributions of $3l3l'$ resonances in the calculations of the electron differential inelastic cross sections $d\sigma/(d\Omega)$ for $C^{5+}(1s)$ have been considered.

*Also at CONICET, Argentina.

†Permanent address: J. R. Macdonald Laboratory, Department of Physics, Kansas State University, Manhattan, KS 66506.

The calculations are simplified because of the observation that for $e^- + C^{5+}(1s)$ collisions, all the doubly excited states ($3l3l'$) produced can have only orbital magnetic quantum number M_L equal to zero when the axis of quantization is chosen as the electron-beam direction. Since the different M_L values are not statistically populated, deexcitation of these doubly excited states by electron emission (autoionization) leads to a nonisotropic electron angular distribution. We have calculated this angular distribution $W(\theta)$ for all states belonging to the $3l3l'$ complex (for details, see Ref. [8]), and the resonance strengths $\Omega(2l)$ defined below,

$$\Omega(2l) \equiv \frac{2.475\times 10^{-30}}{E} \frac{(2L_d+1)(2S_d+1)}{2} A_a(d-g) \times \frac{A_a(d-2l)}{\sum A_a + \sum A_r} \text{ cm}^2\,\text{eV} . \quad (1)$$

The doubly excited states, the ground state, and the states for $n=2$ are denoted by d, g, and $2l$, respectively. A_a and A_r are the autoionization rates and the radiative rates in units of s^{-1}. E represents the electron energy, i.e., the difference between the energy of the doubly excited state and the ground state of the initial ion (C^{5+}).

In the impulse approximation, the bound electrons of the target (H_2) are treated as "quasi"-free electrons with a characteristic momentum distribution, where the projectile (C^{5+}) ion velocity is much larger than the typical electron velocity of the target atom.

The differential electron cross section, with final electron energy ε in the projectile frame, can be written in the impulse approximation (in units of cm^2/sr) as

$$\frac{d\sigma}{d\Omega}(d\rightarrow 2l,\varepsilon,\theta) = \Omega(2l)W(\theta)\left[\frac{J(Q)}{(Q+V_p)\varepsilon_0}\right] , \quad (2)$$

where

$$Q \equiv (2E+2E_I)^{1/2} - V_p . \quad (3)$$

The Compton profile of the target (H_2), $J(Q)$, Q, and the velocity of the projectile V_p are in a.u., $\varepsilon_0 = 27.21$ eV, and E_I is the electron-binding energy of H_2. The normalized angular distribution of the electron is $W(\theta)$.

The differential electron cross section in the laboratory frame, with electron energy ε_L and observation angle θ_L, is given by standard transformations,

$$\frac{d\sigma_{\text{lab}}}{d\Omega}(\varepsilon_L,\theta_L) = \frac{\varepsilon_L}{\varepsilon}\left[1-\frac{t\sin^2\theta_L}{\varepsilon}\right]^{-1/2} \times \frac{d\sigma}{d\Omega}(d-2l,\varepsilon,\theta) , \quad (4)$$

where

$$\varepsilon_L = [t^{1/2}\cos\theta_L + (\varepsilon - t\sin^2\theta_L)^{1/2}]^2 , \quad (5a)$$

$$\cos\theta = \frac{V_p - (2\varepsilon_L)^{1/2}\cos\theta_L}{[2\varepsilon_L + V_p^2 - 2V_p(2\varepsilon_L)^{1/2}\cos\theta_L]^{1/2}} . \quad (5b)$$

The cusp energy t is equal to $\frac{1}{2}V_p^2$.

All the calculations were performed using the Hartree-Fock atomic model with the inclusion of electron-configuration mixing in the same complex.

III. EXPERIMENT

The experiment was performed at the 6-MV Aarhus tandem accelerator. The general characteristics of the experimental setup have been described before [13], and only details important for the present experiment will be given here (see also Fig. 1). The beam is collimated by a set of three fixed apertures. Immediately after the third aperture, the beam traverses a differentially pumped gas cell. The emitted electrons as well as the ion beam exit the gas cell through a 10°-wide forward window. The electrons are analyzed by a 45° parallel-plate analyzer with a theoretical resolution of 0.25% and detected by a channel-electron multiplier. The ion beam is collected by a Faraday cup (FC) placed in front of the analyzer. The minimum electron-observation angle is 0.8°, which is determined by the size and distance between the collimators and the first entrance slit of the analyzer. Due to the minimum electron-observation angle and the design of the FC, electrons between 1° and 6.5° could be detected. Very low background of electrons from the residual gas and from the ion beam was observed even for the smallest observation angle.

Figure 2 shows the electron spectrum obtained at 1°. In Fig. 2(a), a wide range of electron energy is shown. The large peak on the left-hand side is the electron-capture-to-the-continuum (EC) peak [14], and the broad peak on the right-hand side is the binary-encounter (BE) peak [1]. On top of the BE peak, Auger electrons from the resonant configurations $2lnl'$ are observed. The energy of these Auger lines is well known [5] and has been used to obtain the beam energy. This procedure is found to be more accurate than to obtain the beam energy from the EC peak, which in the present experiment cannot be measured at 0°.

Auger electrons are observed on the right-hand side of the EC peak, around 600 eV. An expansion of this energy region is shown in Fig. 2(b). Figure 2(b) is not an enlargement of Fig. 2(a), but refers to another measurement where the analyzer voltage is scanned within an interval corresponding to the energy of the Auger electrons emitted from the $3lnl'$ doubly excited configurations of C^{4+}. The series $3l3l', 3l4l', 3l5l', 3l6l', \ldots$ are clearly seen in Fig. 2(b). Another expansion of the electron spectrum within the energy range of the Auger electrons corresponding to the $3l3l'$ doubly excited configuration of C^{4+} is shown in Fig. 2(c).

Since the acquisition of each electron spectrum re-

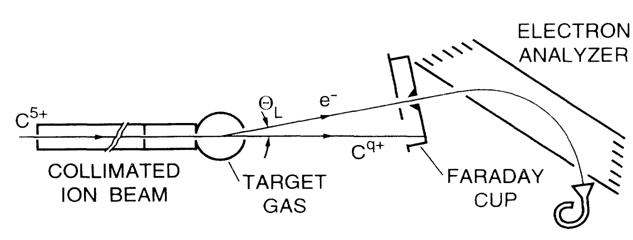

FIG. 1. Experimental setup.

quires a prolonged measurement, the long-term energy stability of the accelerator is extremely important. Therefore, great care was taken in running the accelerator in a very stable mode. The Aarhus tandem accelerator is updated for the ^{14}C-dating program, and its stability has recently been studied by measuring very narrow nuclear resonances [15]. The spectrum shown in Fig. 2(c) is the result of measuring for 12 h. The observed resolution is 0.4%, which, compared to the theoretical 0.25%, demonstrates that the effect of beam-energy drifting is small in the present experiment.

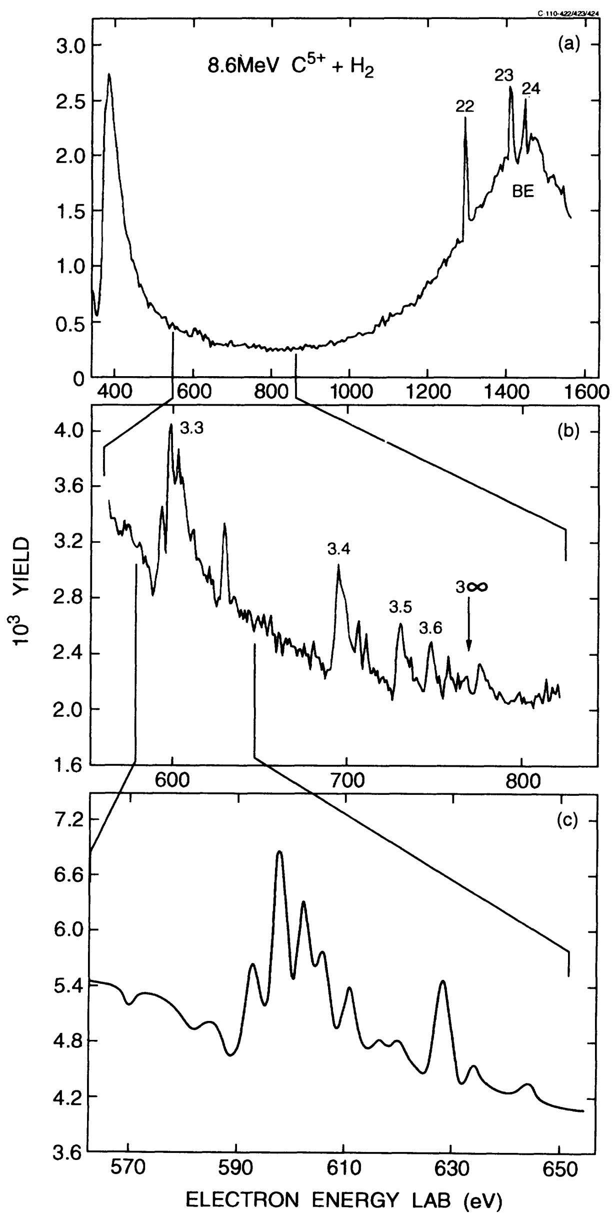

FIG. 2. Electron spectra observed at 1° observation angle from the collision 0.712 MeV/u $C^{5+}+H_2$. (a) Wide energy range showing the EC peak, the BE peak, and Auger lines from resonant configurations $2lnl'$; (b) energy range showing Auger lines from the configurations $3lnl'$; (c) same as (b) for $3l3l'$ states. (b) and (c) are not expansions of (a), but other measurements, each with a different scanning voltage range.

IV. RESULTS AND DISCUSSION

In Fig. 3, a schematic-level diagram with possible excitation and deexcitation paths involving doubly excited states is shown. These states are populated as a result of excitation of the 1s electron and simultaneous capture of a quasifree electron from the target. A "schematic" target-electron Compton profile is also shown. The figure further shows how the projectile energy can be calculated to obtain maximum population of the resonances of interest. The present experiment is performed with C^{5+} ions with an energy of 8.6 MeV. This corresponds to an electron distribution with a maximum at ~350 eV, which is not really optimum in the present situation where we aimed at 400 eV. However, we have not considered the energy shift in the binary-encounter peak described by González *et al.* [16]. As can easily be seen from Fig. 3, we expect to populate $2lnl'$ and $3lnl'$ states and possibly higher-excited states.

The Auger lines corresponding to decay of the doubly excited $3l3l'$ states were fitted by a least-squares method, using a Gaussian shape and a linear-background function. An example of a fitting is shown in Fig. 4. The former line, corresponding to the $3s^2\,{}^1S$ state, is affected by a Fano-type interference, which is not included in the fit. The spectra obtained for observation angles ranging from 1° to 5° have been fitted using a nine-peak structure. A ten-peak structure could also be fitted but with a higher statistical χ^2 and with a nonsatisfactory fit over the full angular range studied. Therefore, the nine-peak

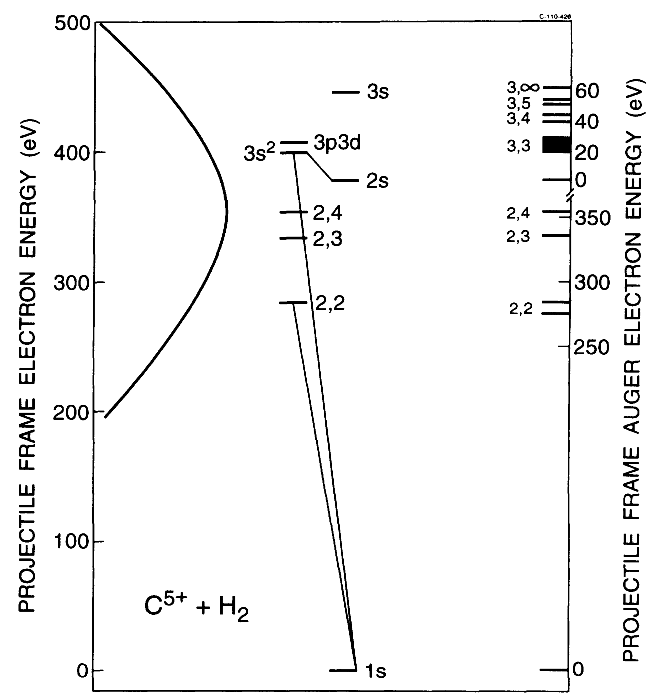

FIG. 3. Energy-level diagram for doubly excited C^{4+} and some excitation and deexcitation paths of relevance to the present experiment. Also shown is a schematic energy distribution of target electrons relative to a 8.6-MeV C^{5+} ion. The projectile-frame energy of Auger electrons is shown on the vertical scale to the right.

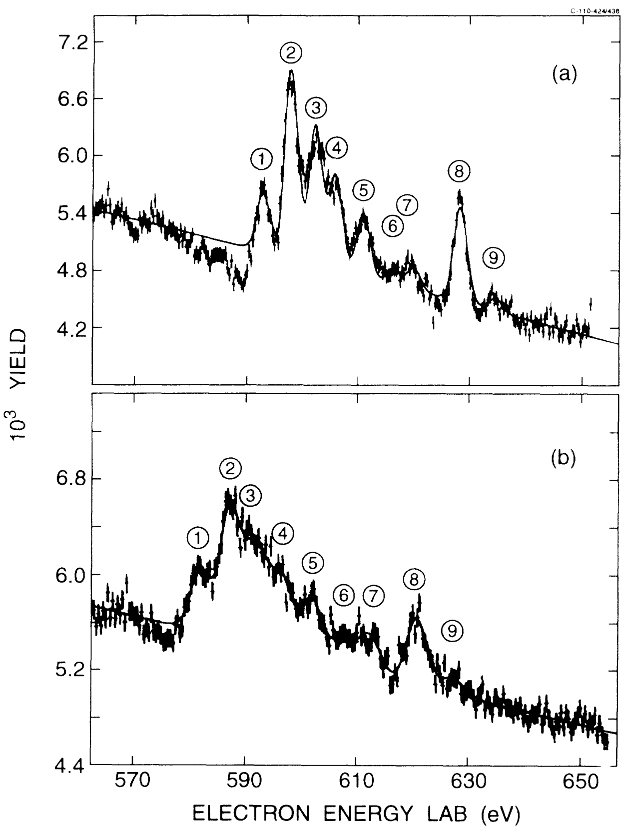

FIG. 4. Electron spectra from decay of $3l3l'$ configurations fitted with a nine-peak structure, as shown in Table I, corresponding to observation angles (a) 1° and (b) 4°.

structure was chosen to be the most suitable. In all the fits, the width and the energy position were free parameters. The width was, as expected, found to increase linearly with the emission angle in the range 1°–5° due to Doppler broadening. Leaving the peak positions free and obtaining the same peak structure along the different angles ensure the consistency of the method, with the low-intensity peak 6 as the only exception. Note that for 4° observation angle [Fig. 4(b)], the position of the fitted peak 6 relative to the others has changed, most likely because of bad statistics. For this reason, we have excluded the peak from the analysis below.

Table I shows the measured energy positions and the relative intensities of the $3l3l'$ series. The different theoretical values are from van der Hart and Hansen [17] (theor. 1), and the present theory (theor. 2). The experimental and theoretical relative intensities are normalized to the second peak $3p^2\,{}^1D$.

Excellent agreement between the experimental values and theory 1 [17] for the energy positions is found. Two lines (4 and 6 in Fig. 4 and Table I) are well identified as transitions from the triplet states $3s3d\,{}^3D$ and $3p3d\,{}^3P$. Theory 2 gives a good estimate of the relative energy position of most of the lines, but it shows a constant shift towards lower energies of about 1.3 eV.

To get the experimental relative intensities, the areas of the Gaussian peaks after background subtraction were normalized to the beam integration and to the pressure in the gas cell. The statistical errors are given by the standard deviation of the area in the fit, which is in the range of 2–15 %. The uncertainty in the determination of the gas pressure introduces an extra error of about 2% in all cases.

By measuring at angles from 1° to 5° in the laboratory frame, a broad interval of scattering angles (from 5° to 30°) in the projectile frame is covered. The scattering angles in the projectile system are related to laboratory ones through Eq. (5b). In Fig. 5, the measured angular dependence for eight of the peaks described in Table I is compared with theoretical estimates. Peak 6 is not clear in all the spectra, and its angular dependence could not be studied. Theory and experiment are normalized to each other at 0° for the $3p^2\,{}^1D$ line. In most cases, the agreement between theory and experiment is good. However, for the triplet $3s3d\,{}^3D$ (peak 4) and the singlet $3p3d\,{}^1F$ (peak 7), we observe a large discrepancy between the data and the Hartree-Fock calculations. A large basis set for the $3p3d\,{}^1F$ and $3s3d\,{}^3D$ state was used to obtain the autoionization rates. The total rates are found to be sensitive to these considerations, but the autoionization rate to the ground state $A_a(d-g)$ in Eq. (1) does not change

TABLE I. Energy positions and relative intensities of Auger electrons resulting from doubly excited states $3l3l'$ of C^{4+}. Peak numbers label the nine peaks identified in the present experiment. Theor. 1 corresponds to Ref. [17] and Theor. 2 to the present work (see Sec. II). The relative experimental intensity of 94 should be considered the sum of the $3s3p\,{}^1P$ and $3s3d\,{}^3F$ states.

Peak		Energy (eV)			Rel. intensities	
no.	Terms	Expt.	Theor. 1	Theor. 2	Expt.	Theor. 2
1	$3s^2\,{}^1S$	21.45	21.45	20.7	42	20
2	$3p^2\,{}^1D$	22.48	22.54	21.5	135	135
3	$3s3p\,{}^1P$	23.39	23.45	22.4	94	19
	$3p3d\,{}^3F$	23.39		22.4		61
4	$3s3d\,{}^3D$	24.14	24.21	23.0	65	20
5	$3d^2\,{}^1D$	25.14	25.36	24.5	45	25
6	$3p3d\,{}^3P$	25.94	25.82		8	
7	$3p3d\,{}^1F$	27.02	27.27	26.8	24	94
8	$3s3d\,{}^1D$	29.08	28.95	29.3	68	71
9	$3p3d\,{}^1P$	29.91	29.91	30.3	12	11

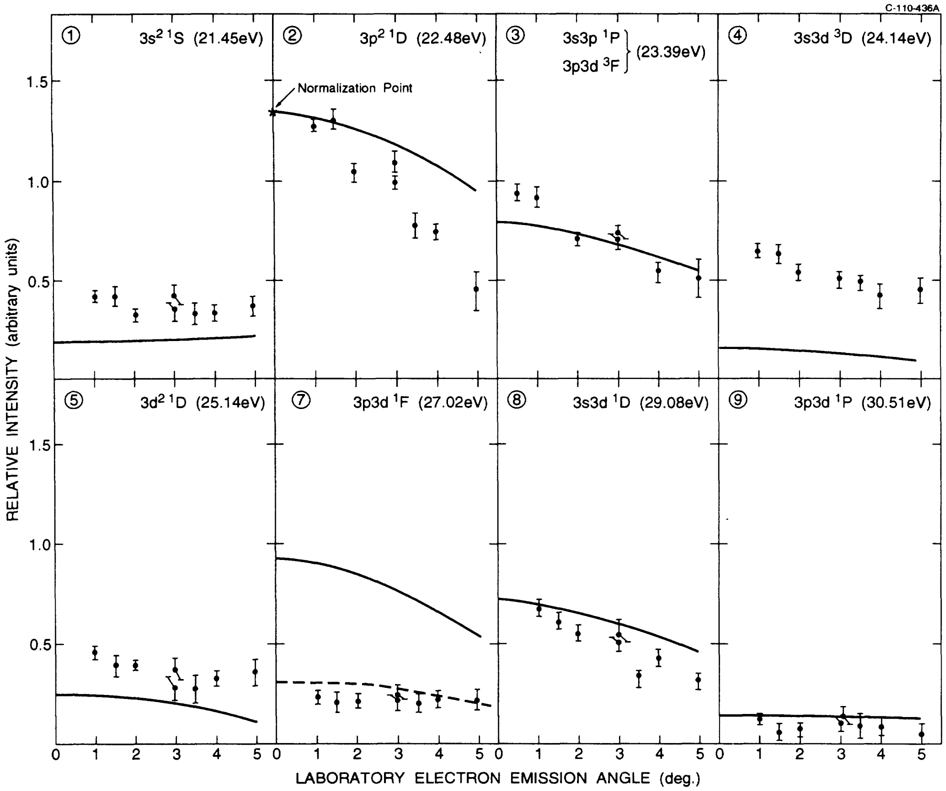

FIG. 5. Intensities of peaks described in Table I as a function of laboratory scattering angle. The solid line is the result of the present theory normalized to peak 2 at 0°. The error bars include only statistical errors derived from the fit. The dashed line for the $3p3d\ ^1F$ state is calculated using the autoionization rate to the ground state from Ref. [17].

significantly. There is, however, a significant difference between $A_a(d-g)$ values in the present calculations and the truncated-diagonalization method [17] for the $3p3d\ ^1F$ state. Figure 5 contains the theoretical results for the ^1F state, using both values of $A_a(d-g)$. It is likely that the value of $A_a(d-g)$ for the $3s3d\ ^3D$ state may be similarly influenced by strong electron-correlation effects. Neither peak is associated with the most dominant transitions, and the error bars are larger. Nevertheless, for peak 4, the calculation overestimates the data by a factor of 3 at 1° observation angle. This discrepancy is too large to be explained as statistical uncertainties or as a consequence of lack of resolution. It should be noted that a comparison between experiment and theoretical calculations of relative line intensities is not straightforward. The data may be influenced by state mixing, and also interferences with the direct nonresonant channel most likely make problematic a detailed comparison of line intensities based on the present measurements and theory. The spectrum shown in Fig. 4 indicates that peak 1 has a resonance structure (Fano profile), and accordingly, the Gaussian-peak area is not an accurate measure of the line intensity related to the population of the $3s^2\ ^1S$ state. Similar effects may influence some of the other lines.

V. CONCLUSION

Auger electrons emitted after collisions between C^{5+} and H_2 have been measured as a function of emission angle. A detailed experimental and theoretical investigation of electrons resulting from decay of doubly excited states $3l3l'$ of C^{4+} is presented. The line energies are in good agreement with calculations based on the truncated-diagonalization method by van der Hart and Hansen [17]. The relative intensities and angular dependence of the states within the $3l3l'$ manifold are compared to a calculation using the Hartree-Fock model (see Sec. II). This calculation compares well for the angular dependence of most of the Auger lines. However, a large deviation is found for two states, $3s3d\ ^3D$ and $3p3d\ ^1F$. There is evidence for strong electron correlation for the $3p3d\ ^1F$ state autoionization rate to the ground state. When this rate, calculated with the truncated-diagonalization method [17], is used in the present calculations, the agreement between theory and experiment is excellent. It is probable that the $3s3d\ ^3D$ autoionization rate to the ground state may be influenced also by electron-correlation effects. Further investigations, using higher resolution and a better theoretical model than the Hartree-Fock model, could settle that question for the $3s3d\ ^3D$ state.

ACKNOWLEDGMENTS

One of us (C.P.B.) was supported by the Division of Chemical Sciences, Office of Basic Energy Sciences, Office of Energy Research, U.S. Department of Energy, and A.D.G. acknowledges support from Aarhus University. We thank Professor J. E. Hansen for providing the $3p3d\ ^1F$ autoionization rate.

[1] D. H. Lee, P. Richard, T. J. M. Zouros, J. M. Sanders, J. L. Shinpaugh, and H. Hidmi, Phys. Rev. A **41**, 4816 (1990).
[2] P. D. Fainstein, H. V. Ponce, and R. D. Rivarola, Phys. Rev. A **45**, 6417 (1992), and references therein.
[3] A. Itoh, T. J. M. Zouros, D. Schneider, U. Stettner, and N. Stolterfoht, J. Phys. B **18**, 4581 (1985).
[4] N. R. Badnell, Phys. Rev. A **41**, 3555 (1990).
[5] D. H. Lee, P. Richard, J. M. Sanders, T. J. M. Zouros, J. L. Shinpaugh, and S. L. Varghese, Phys. Rev. A **44**, 1636 (1991), and references therein.
[6] B. D. De Paola, R. Parameswaran, and W. J. Axmann, Phys. Rev. A **41**, 6533 (1990).
[7] M. Schulz *et al.*, Phys. Rev. Lett. **62**, 1738 (1989).
[8] C. P. Bhalla, Phys. Rev. Lett. **64**, 1103 (1990).
[9] G. Kilgus *et al.*, Phys. Rev. Lett. **64**, 737 (1990).
[10] D. C. Griffin and M. S. Pindzola, Phys. Rev. A **35**, 2821 (1987).
[11] T. J. M. Zouros, in *Recombination of Atomic Ions,* Vol. 296 of *NATO Advanced Study Institute Series B: Physics,* edited by W. G. Graham, W. Fritsch, Y. Hahn, and J. A. Janis (Plenum, New York, 1992), p. 271.
[12] Y. Hahn and K. J. La Gattuta, Phys. Rep. **166**, 195 (1988).
[13] A. D. González, P. Dahl, P. Hvelplund, and K. Taulbjerg, J. Phys. B **25**, L573 (1992).
[14] P. Dahl, J. Phys. B **18**, 1181 (1985).
[15] A. D. González and E. Horsdal Pedersen, Nucl. Instrum. Methods B **71**, 22 (1992).
[16] A. D. González, P. Dahl, P. Hvelplund, and P. D. Fainstein, J. Phys. B **26**, L135 (1993).
[17] H. W. van der Hart and J. E. Hansen, J. Phys. B **26**, 641 (1993); (private communication).